This is the Pre-Published Version.

S. Lin, Y. Qin, X. Huang, M. Gollner (2023) *Use of Pre-Charred Surfaces to Improve Fire Performance of Wood*, **Fire Safety Journal**, 103745. https://doi.org/10.1016/j.firesaf.2023.103745

Use of Pre-Charred Surfaces to Improve Fire Performance of Wood

Shaorun Lin [a,b], Yunzhu Qin [a,c], Xinyan Huang [a,*], Michael Gollner [b]

[a]*Research Centre for Fire Safety Engineering, Department of Building Environment and Energy Engineering, the Hong Kong Polytechnic University, Kowloon, Hong Kong*

[b]*Department of Mechanical Engineering, University of California, Berkeley, CA, USA*

[c]*The Hong Kong Polytechnic University Shenzhen Research Institute, Shenzhen, Guangdong, China*

*Corresponding to xy.huang@polyu.edu.hk (X. Huang)

Abstract: Wood is one of the most commonly-used and sustainable construction materials, but it is flammable in nature. Pre-charring is an ancient approach used to protect wooden construction materials against biochemical impacts, but its effectiveness in improving fire performance is still poorly understood. This work proposes a novel method to generate engineered wood with a uniform and robust surface char layer through slow pyrolysis under low thermal irradiation of 20 kW/m^2. We found that the flammability of the pre-charred wood can be significantly reduced under higher irradiations up to 50 kW/m^2 by increasing the ignition time by up to seven-fold and doubling the ignition temperature to about 670 ºC. For the tested wood species (Merbau), we quantify a minimum char-layer thickness of 6 ± 1 mm to achieve effective fire retardancy. The fire hazards of pre-charred wood are also mitigated significantly, where observed flames become weaker, thinner, and bluer than that of the virgin wood. The peak heat release rate of burning pre-charred wood is reduced by over 50%, helping maintain the fire resilience of timber structures. This work quantifies the fire performance of pre-charred wood, highlighting a promising direction toward fire-safe timber construction materials.

Keywords*: timber building; reaction to fire; fire retardancy; sustainable construction; material flammability; ignition*

1. Introduction

The use of wood has significantly contributed to the development of human civilisation and it has been adopted as one of the longest-standing construction materials for more than 10,000 years [1,2]. For example, the world's oldest surviving wooden building, the Horyuji Temple near Nara, Japan, was constructed at least 1,300 years ago [3] (Fig. 1a). Despite the long-lasting history of wooden construction and timber buildings, steel and concrete have dominated large-occupancy construction since the industrial revolution. Nevertheless, over the past few decades, wood has experienced a renaissance, recognizing its benefits as a green and renewable construction material for high-rise buildings, aiming to pave the way for a future carbon-neutral world [4–8]. Compared with modern construction materials such as steel, concrete and glass, the production processes of natural and engineered wood products require lower energy consumption and emit less carbon [9,10]. In recent years, the mushrooming interest in high-rise timber buildings has marked a firm commitment to innovation, sustainability and modernity by combining the vision of ecological and innovative

architectures [7,11]. For example, the new 84-meter, 24-story high 'HoHo Tower' in Vienna, Austria (Fig. 1b), is the world's latest milestone of the tallest timber skyscraper.

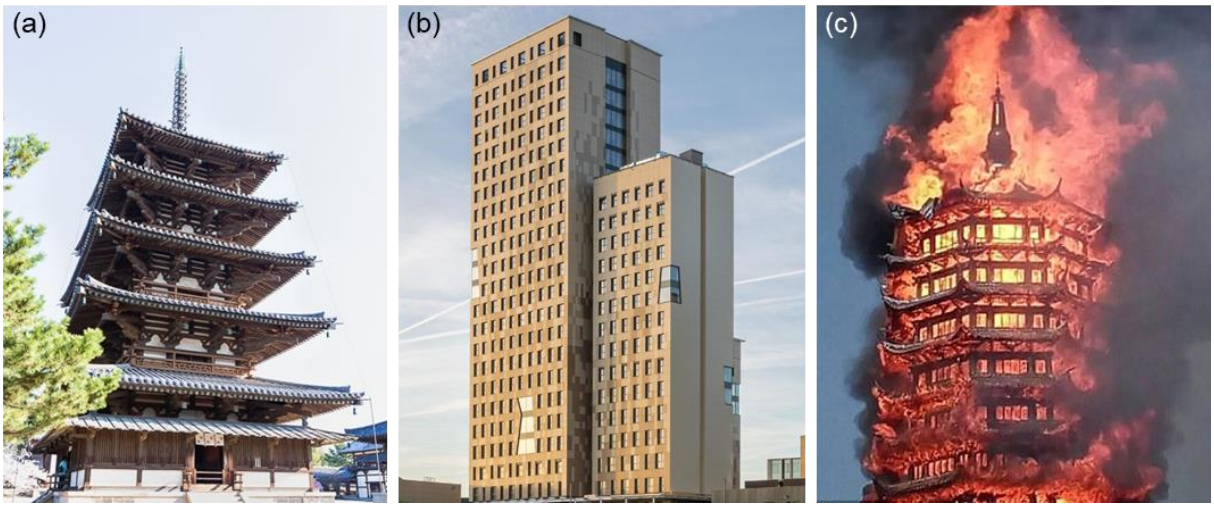

Fig. 1. Photos of (a) the Horyuji Temple near Nara, Japan (Credit: Rhonda Krause), (b) the HoHo Tower in Vienna, Austria (Credit: HoHo Vienna/Michael Baumgartner/Kito), and (c) the Lingguan Tower engulfed in flames in 2017 (Credit: AsiaWire).

Wood is an inhomogeneous and anisotropic natural composite made of hemicellulose and cellulose that is strong in tension and embedded in a matrix of lignin that resists compressive strength [12–14]. However, due to the flammable nature of the wooden material, except for cost, supply and issues of moisture control during its lifetime, the fear of fire is probably the single largest contributor to the abandonment of wood as a construction material in large buildings [15–17]. For example, the 16-story Lingguan Tower in China, which was the tallest wooden pagoda in the world, burnt completely to the ground after being engulfed in flames for around 4 hours (Fig. 1c). Despite new fire retardants and active and passive fire prevention techniques [18], a continuous series of fire accidents raises the issue of fire safety as a key public concern. As a result, strict fire safety and structural requirements increase building costs and limit wood's practicality as a building material [19]. Therefore, it is urgent for the scientific community to improve our understanding of the fire dynamics of wooden materials and thus improve their fire resilience for future timber structures.

As a typical charring material, wood can sustain both flaming and smouldering combustion [20]. The fire dynamics of wooden materials have been extensively studied, revealing many insights into the phenomenon of ignition [21–24], fire spread [25–27], deformation [14,28,29], and extinction [30–36]. Methods that may improve the reaction to fire of wooden materials have also been well explored, especially the application of fire-retardant systems [37–46]. The mechanisms of these fire-retardant systems include endothermic degradation (e.g., magnesium and aluminium hydroxides) [43], thermal shielding (e.g., intumescent additives) [47], dilution of gas fuels (e.g., inert gas produced by thermal degradation) [48], and gas-phase radical quenching (e.g., chlorinated and brominated materials) [42].

For example, intumescent coatings are an effective method to reduce material flammability by producing a massive volume expansion resulting in a porous charred surface layer, insulating the flammable material underneath [42,49]. Additionally, chemical modifications impregnated into wooden materials have offered an alternative to provide protection against water, corrosion, ultraviolet and thermal degradation (fire), showing excellent application prospects [50].

Charring is a historically-used approach to generate a protective surface layer on wood resistant to biochemical impacts [51–53]. During the first century BC, Vitruvius, a Roman architect and engineer, recommended using carbonisation to increase the service life of bridges and fortification fences [42]. In the 1600s, the technique of 'charring wood' was further developed in Japan to improve biological resistance and fire-harden the fast-growing wooden structures, known as 'shou sugi ban', 'sugi ban' or 'yakisugi' [51,54]. Recently, several studies have been performed to investigate the surface characteristic of charred woods. For example, Kymalainen et al. [55,56] introduced charring on a wood surface using a hot plate and found that treated spruce sapwood exhibits promising characteristics in terms of reduced sorption. Machova et al. [52] also concluded that charring at a particular temperature and duration improved the properties of beech wood such as discolouration and surface roughness. Moreover, the charring process is also believed to improve the fire retardancy of wood materials due to the lower thermal conductivity of char compared to virgin wood [57].

During real fire scenarios, a char layer will be formed on the fire-exposed surfaces and its thickness will grow as the fire progresses [58]. The char layer not only can hold a high temperature, but its porous structure also creates the effective insulation that protect the remaining uncharred residual wood from flame [32,59]. However, for wooden materials with pre-charred surfaces, few studies have evaluated their fire performance. Hasburgh et al. [51] tested several commercial 'shou sugi ban' samples but found that the thin char layer did not systematically improve the fire performance of the wooden materials. Machova et al. [52] suggested that charring should be conducted at a suitable combination of temperature and time to form an effective char layer against fires. Gan et al. [60] generated an insulating char layer on densified wood in a tube furnace at 500 ^{o}C that doubled the ignition time and decreased the maximum heat release rate, but the thickness of the char layer was not mentioned. Therefore, our understanding of the flammability of the pre-charred wood and the required char-layer thickness for an effective protective layer against fires are still limited, requiring more fundamental research and quantitative analyses.

Herein, we develop a novel and low-cost strategy to generate a controllable and uniform char layer over a wood surface under low irradiation of 20 kW/m^2. The thickness of the char layer is accurately controlled by the irradiation duration (0-20 min). The fire performance (flammability or reaction-to-fire behaviour) of the pre-charred wood is evaluated in terms of piloted ignition delay time, ignition temperature, and fire heat release rate under irradiation up to 50 kW/m^2 that simulates real fire scenarios.

2. Experimental details

2.1. Virgin wood sample

The virgin wood sample used in this work is Merbau wood from Southeast Asia (Fig. 2), and its dry bulk density was measured to be around 900 kg/m^3. Initially, the wood samples were uniformly cut into dimensions of 10 cm × 10 cm × 3 cm. To prevent cracking due to high-temperature heating, the wood samples were oven-dried at a low temperature of 50^{o}C for at least 48 h, and then placed into an electronic dry cabinet to avoid the re-absorption of moisture from the ambient [35]. The thermogravimetric analysis (TGA) was conducted using a PerkinElmer STA 6000 Simultaneous Thermal Analyzer at a heating rate of 30 K/min in both air and nitrogen flows, and the representative data are shown in the Appendix. TGA results of char show negligible pyrolysis reaction in Fig. A1b.

2.2. Controlled surface charring process

The charring process was performed using the cone calorimeter (FTT I-Cone Plus) [61,62], which mainly consists of a conical heater, a sample holder and a precision scale. The conical heater provides a relatively constant and even irradiation to the sample area of 10 cm × 10 cm, thus ensuring that the whole exposed surface of the wood sample receives uniform irradiation [35,61]. The periphery of the wood sample was wrapped by a 1-cm thick insulating fiber insulation layer, which reduced lateral heat losses and promoted a steady 1-D charring process perpendicular to the top surface (see Fig. 2).

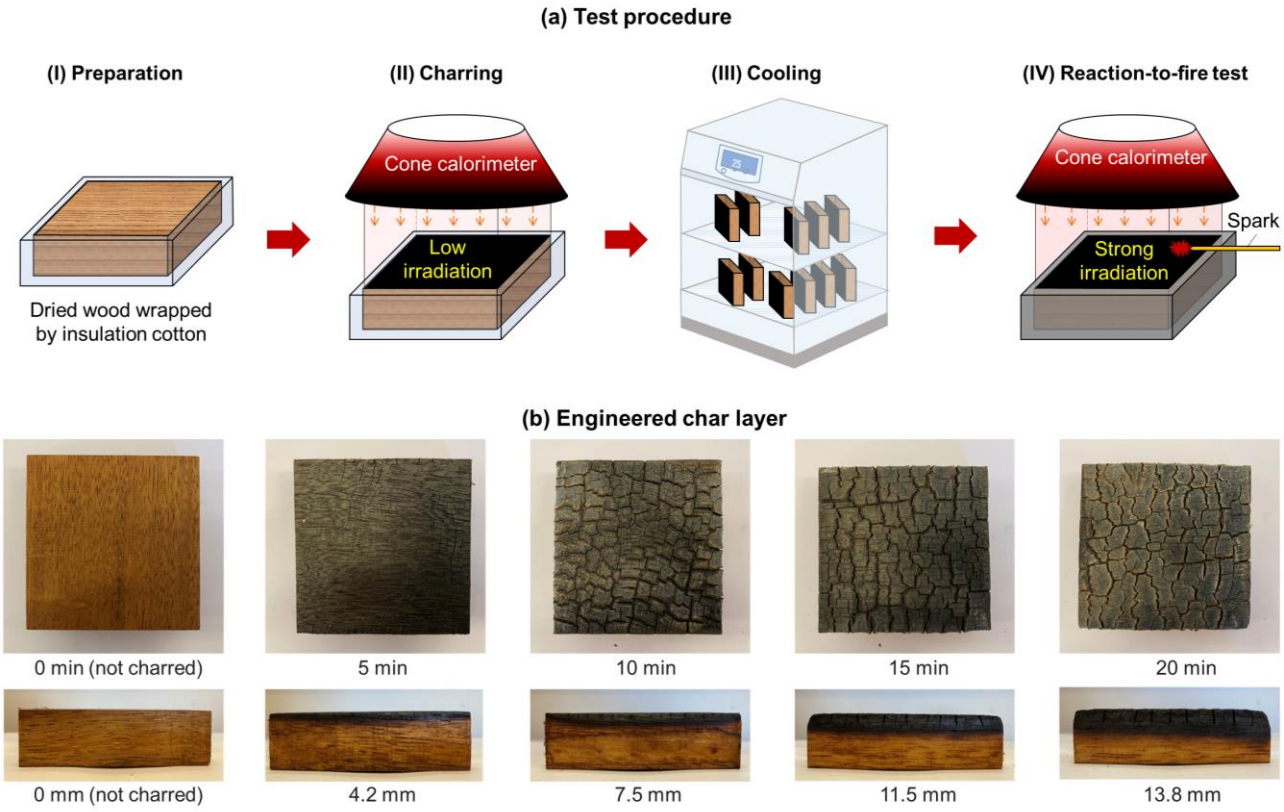

Fig. 2. (a) Schematic diagrams of test procedures, and (b) photos of the wood's top surface (top) and cross-section (bottom) with charring applied for 0 min, 5 min, 10 min, 15 min and 20 min.

The charring irradiation was adjusted to a relatively low level of 20 kW/m^2 which was measured by a radiometer. After that, irradiation was shielded by two steel panels (i.e., a shutter), and the sample was installed on a precision scale where the top unwrapped surface was exposed to the conical heater. Once the steel shield was removed, the prescribed irradiation was applied to the exposed wood surface. The charring duration lasted for 5 min, 10 min, 15 min and 20 min (Video S1), respectively. After charring, some shallow and random fissures were observed on the charred surfaces [63,64], and a uniform char layer was observed on the cross-section of the charred wood samples (see Fig. 2b).

Figure 3 summarises the thicknesses of the pre-charred layers (δ_c) with different charring durations (t_c). As expected, the thickness of the char layer increases almost linearly with the charring duration, with a near-constant charring rate of 0.7 mm/min, consistent with the data in the literature [65]. For example, as the charring duration increases from 5 min to 20 min, the thickness of the charred layer increases from 4.2 mm to 13.8 mm. An empirical correlation between the thickness of the charred layer [mm] and the charring duration [min] was found to be $\delta_c = 0.7t_c$ with R^2=0.99. Note that the charring rate of the wood may vary with the wood species and densities, and the charring rate may decrease if the char layer further expands [65]. Fig. 3(b) further summarises the total mass loss per unit area after the charring process (m_C''), which also increases with the charring duration. For example, as the charring duration increases from 5 min to 20 min, the mass loss per unit area increases from 0.95 kg/m^2 to 6.7 kg/m^2. After charring, the samples were placed into a cabinet for cooling under dry ambient conditions.

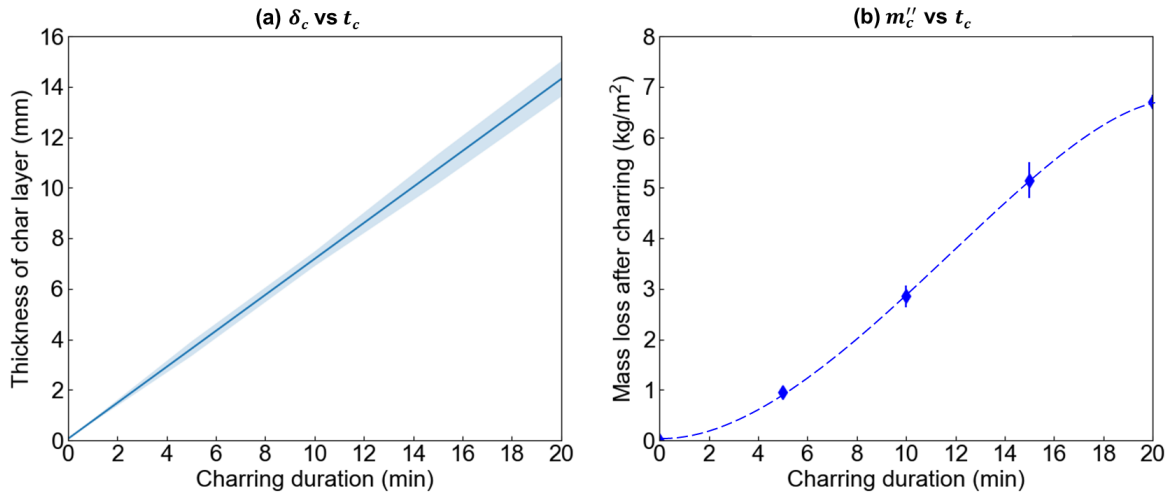

Fig. 3. Relationship between the thickness of a charred layer and charring duration, where a linear fit shown is $\delta_c = 0.7t_c$ with R^2=0.99, and (b) a relationship between the total mass loss per unit area and charring duration.

2.3. Reaction-to-fire test

The standard reaction-to-fire test was conducted using the same cone calorimeter under higher irradiations of 40 kW/m^2 and 50 kW/m^2 following ASTM E1354 and ISO 5660 [61]. The pre-charred wood samples were installed in a stainless-steel sample holder to prevent any edge or curvature effect, as recommended by [61]. The pilot source (a spark) was placed 15 mm above the top surface of the

sample during the heating. Piloted ignition is defined here as the initiation of flaming combustion in the vicinity of a small pilot source located in the boundary layer [66]. Once a flame was piloted, the igniter was removed while the heating was continued to measure the burning rate and fire heat release rate until flame extinction. The surface temperatures of the samples were carefully monitored using two K-type thermocouples (0.5-mm bead diameter) that were closely attached to the top surface [35]. The testing procedure was fully recorded by a side-view camera. During the test, the ambient temperature was maintained at 25 ± 2℃, while the relative humidity was kept at 50 ± 5%. For each test, at least three repeating experiments were performed for uncertainty analysis.

3. Results and Discussion

3.1. Fire phenomena

Figure 4 shows some typical examples of the piloted flaming ignition processes of the wood samples with different thicknesses of pre-charred layers under an irradiation of 40 kW/m^2, where the original videos can be found in the Supplemental materials (Video S2). For the virgin wood (Fig. 4a), once exposed to irradiation, dense smoke was always observed, which could be a mixture of pyrolysis gases and condensed water vapour [67]. After being heated for about 48 s, a typical buoyancy-controlled strong yellow flame was successfully piloted and maintained above the wood surface.

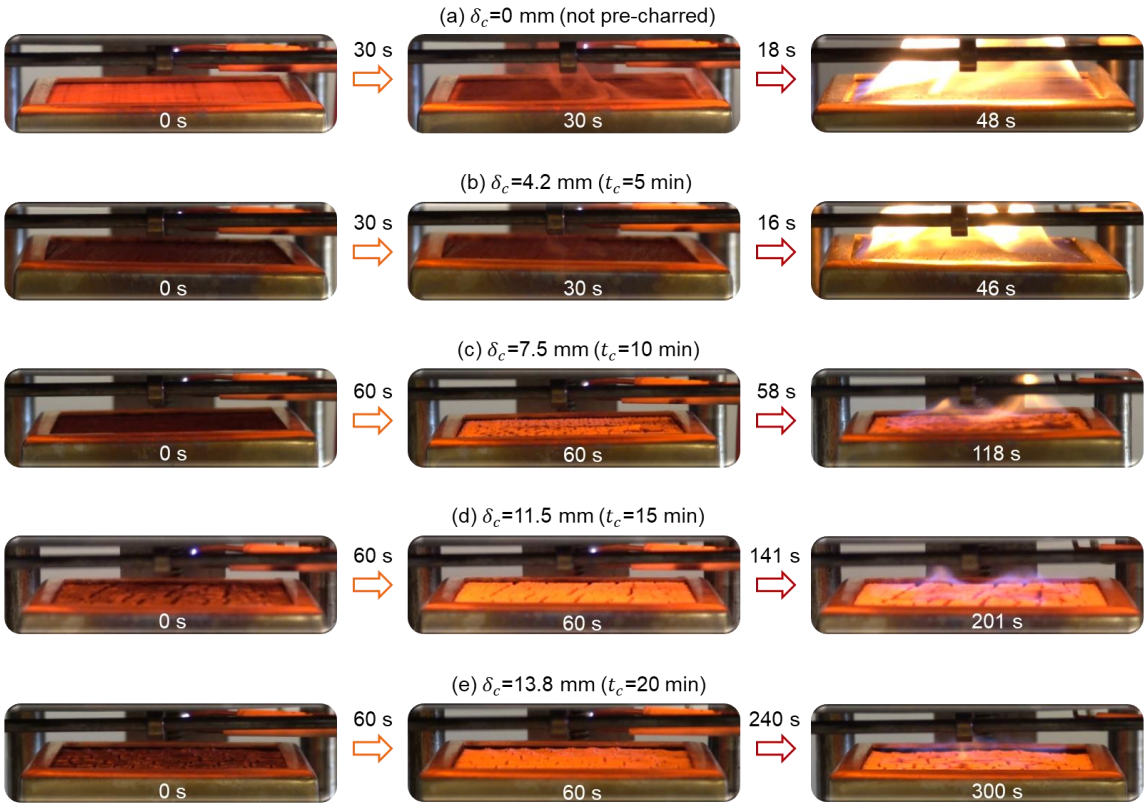

Fig. 4. Snapshots of piloted flaming ignition of wood samples under irradiation of 40 kW/m^2, where the thicknesses of char layers are (a) 0 mm without charring, (b) 4.2 mm with 5-min of charring, (c) 7.5 mm with 10-min of charring, (d) 11.5 mm with 15-min of charring, and (e) 13.8 mm with 20-min of charring (Video S2).

For the wood with a 4.2-mm char layer (Fig. 4b), although less smoke was observed during heating, a strong yellow flame was also piloted at about 46 s, similar to that of virgin wood. Thus, a char layer with a thickness of 4.2 mm is not effective to improve the fire retardancy or reduce the flammability of wood materials (see Sections 3.2 & 3.3).

By increasing the thickness of the char layer to 7.5 mm (Fig. 4c), although a glowing process was first achieved on the char surface, no visible smoke was observed during the heating process. After being heated for about 118 s, a flame was also piloted, but the ignition was delayed by 70 s compared to that of virgin wood in Fig. 4a. Meanwhile, the flame height was decreased due to a smaller fuel burning mass flux (see more discussion in Section 3.5) and the flame intensity also weakened (see more discussion in Section 3.4). Therefore, the general fire performance of wood appears well improved by the pre-charred surface. Further increasing the char thickness to 11.5 mm and 13.8 mm, compared with the virgin wood, the flaming ignition was further delayed by about 150 s and 250 s, respectively.

Moreover, after ignition, only a weak, thin, flat, blue and discrete flame was observed floating above the hot charred surface, analogous to the near-limit blue flame observed in our previous work [33,35]. As the flame height was very small due to a smaller fuel mass flux (see Section 3.5), the flame was only slightly affected by buoyancy. Note that the temperature of the observed blue flame was not necessarily lower than the yellow flame, whereas it only indicated a lower soot concentration in the flame or soot concentrated away from hotter reacting regions [35].

3.2. Ignition time and thermal inertia

Figure 5(a) summarises the piloted flaming ignition time (t_{ig}) of virgin and pre-charred woods with different thicknesses of char layers under irradiations of 40 kW/m^2 and 50 kW/m^2. As expected, given the thickness of the char layer, the required ignition time decreases with increasing radiant heat flux, agreeing with previous trends in the literature [22]. On the other hand, when the thickness of the char layer is smaller than 6 ± 1 mm, given an irradiation level, the sample's ignitability is insensitive to the thickness of the char layer, as the ignition time is almost the same as that of virgin wood. Therefore, a thin layer of char surface (<6 mm) is not sufficient to protect the underlying virgin wood tested in this study against fires radiating up to 50 kW/m^2.

In terms of conduction heat transfer, the thermal penetration depth (δ_T) is defined as the distance that the heat diffuses through the material during a time [68]. Herein, a char layer thinner than 6 mm does not exceed the thermal penetration depth ($\delta_T \sim \sqrt{8\alpha t_{ig}} \approx \sqrt{8 \times 0.1 \times 40} = 5.7$ mm) of the virgin wood at the ignition moment, where $\alpha \approx 0.1$ mm^2/s is an average thermal diffusivity of wood [66,69]. Comparatively, as the thickness of the char layer exceeds 6 ± 1 mm, the required ignition time starts to increase greatly with the thickness of the char layer. For example, given irradiation of 40 kW/m^2, compared with that of virgin wood (39 s), the ignition time increases by around 5 times to 197 s and 7 times to 272 s, as the thickness of the char layer increases to 11.5 mm and 13.8 mm, respectively. Therefore, an effective char layer could remarkably improve the fire performance (or retardancy) of

wood materials. Note that t_{ig} is proportional to the density of wood (see Eq. 1), while δ_T also varies with t_{ig}. In other words, the minimum char-layer thickness to achieve effective fire retardancy may not be a constant but sensitive to the wood species and density, requiring further investigations.

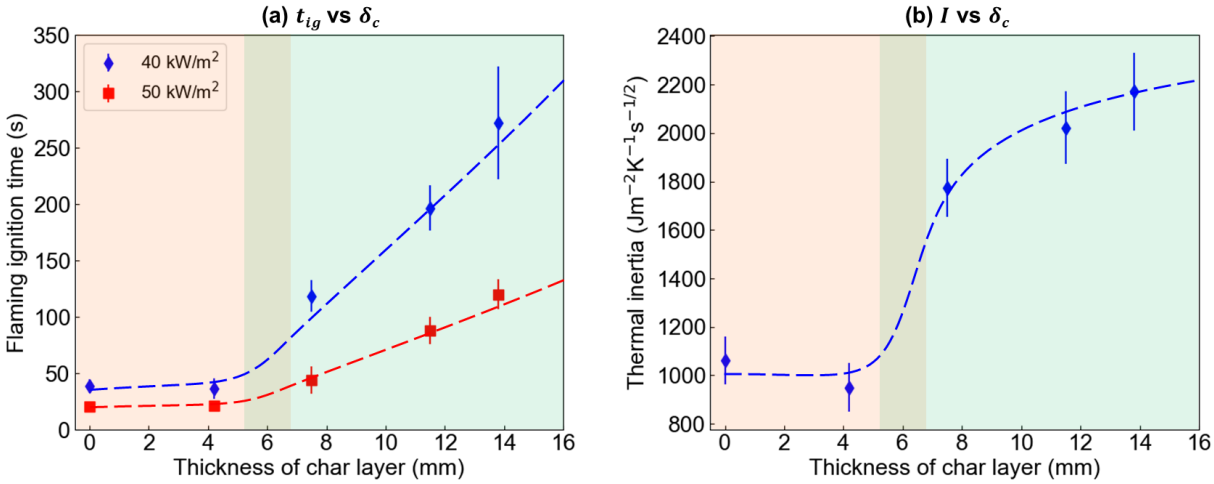

Fig. 5. (a) Piloted flaming ignition delay times under irradiations of 40 kW/m^2 and 50 kW/m^2, and (b) calculated thermal inertia for the virgin and pre-charred woods, where markers represent the average values, error bars represent the standard deviations between experiments, and dashed lines represent a best-fit function.

For a thermally thick fuel where the fuel thickness is generally larger than 2 mm [66], the ignition time (t_{ig}) can be estimated as

$$t_{ig} \approx \frac{\pi}{4} k\rho c \left(\frac{T_{ig} - T_\infty}{\dot{q}''_{ir}} \right)^2 \quad (1)$$

where k, ρ, and c are the thermal conductivity, bulk density and specific heat, respectively; T_{ig} and T_∞ are the ignition temperature (see Section 3.3) and ambient temperature (25 °C); and $\dot{q}''_{ir}$ is the irradiation. As the irradiation increases, the ignition time decreases, agreeing with the experimental observations (Fig. 5a). By rearranging Eq. (1), we can estimate the fuel **thermal inertia** (I) as

$$I = \sqrt{k\rho c} = 2\sqrt{\frac{t_{ig}}{\pi}} \left(\frac{\dot{q}''_{ir}}{T_{ig} - T_\infty} \right) \quad (2)$$

which is a measure of its resilience to external thermal impact [66].

Fig. 5(b) plots the calculated thermal inertia of engineered wood with different thicknesses of char layers. Initially, the thermal inertia of virgin wood is around 1198 J·m^{-2}·K^{-1}·s$^{-1/2}$, similar to existing literature values [66]. However, as the thickness of the char layer increases to 11.5 mm and 13.8 mm, the thermal inertia of the composite increases to 2282 J·m^{-2}·K^{-1}·s$^{-1/2}$ and 2337 J·m^{-2}·K^{-1}·s$^{-1/2}$, improving

the fire performance of wood samples with pre-charred surfaces that insulate the flammable virgin material.

3.3. Ignition temperature and minimum irradiation

To form a thermal ignition criterion, it is a common practice to assume a specific ignition temperature for each material [66]. Flaming ignition is then estimated to occur when the temperature of the fuel surface reaches this critical value; with its utility also useful in theories to predict the fire spread rate [66,67]. For virgin wood, ignition temperature is a theoretical construct that acts as a surrogate for the pyrolysis temperature (at least the temperature at which sufficient pyrolysis occurs for ignition), as defined by the thermal model [66]. Comparatively, the ignition of a pre-charred wood depends on the the temperature below char layer and the in-depth pyrolysis processes. Thus, the recorded top-surface temperature at the moment of ignition is no longer a good indicator or surrogate of the pyrolysis temperature of raw wood. Nevertheless, characterizing the surface temperature at ignition is meaningful in terms of understanding the improvement of fire performance of the pre-charred woods. It is also useful for other analyses such as the flame spread and smoldering fire processes.

Fig. 6 shows some examples of the time evolution of surface temperatures over both virgin and pre-charred wood samples under an irradiation of 40 kW/m^2, where the moments of ignition are indicated by solid circles. Once exposed to the irradiation, the surface temperature rapidly increases, with the rate of increase slowing over time because of an increase in environmental cooling. Finally, at the moment of flaming ignition, the surface temperature experiences a sudden jump, similar to the observations in [67].

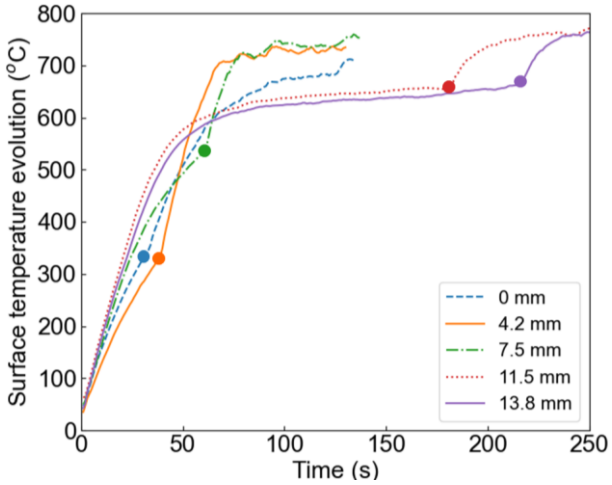

Fig. 6. Examples of surface temperature evolutions of the virgin wood and different pre-charred woods, where the ignition moments are marked by solid circles

Fig. 7(a) further summarises the ignition temperature of virgin and pre-charred wood samples with different thicknesses of char layers. Analogous to the pattern of the ignition time, for the virgin or pre-charred wood samples with a 4.2-mm char layer, the ignition temperatures remain constant at around 350 °C, agreeing with existing literature [66]. However, as the thickness of the char layer exceeds 6

mm, the ignition temperature shows a sudden increase. For example, as the thickness of the char layer increases from 11.5 mm to 13.8 mm, the ignition temperature dramatically increases from 655 °C to 683 °C, which is almost twice the ignition temperature of virgin wood.

For virgin wood, the minimum irradiation required to achieve piloted ignition was measured to be $\dot{q}''_{min} = 13$ kW/m^2. Theoretically, this value should approximately balance the overall environmental heat loss ($\dot{q}''_{loss}$) [66] as

$$\dot{q}''_{min} = \dot{q}''_{loss} = \varepsilon\sigma\left(T_{ig}^4 - T_\infty^4\right) + h\left(T_{ig} - T_\infty\right) \quad (3)$$

where ε is the emissivity, $\sigma = 5.67 \times 10^{-8}$ Jm^{-2}s^{-1}K^{-4} is the Stefan-Boltzmann constant, $h = 1.52\left(T_{ig} - T_\infty\right)^{1/3}$ is the free convection heat transfer coefficient for a horizontal hot plate [66,68]. Fig. 7(b) summarises the calculated minimum irradiation based on Eq. 3 and Fig. 7(a), where the pre-charred wood can resist irradiation above 30 kW/m^2, if the char layer is thicker than 10 mm.

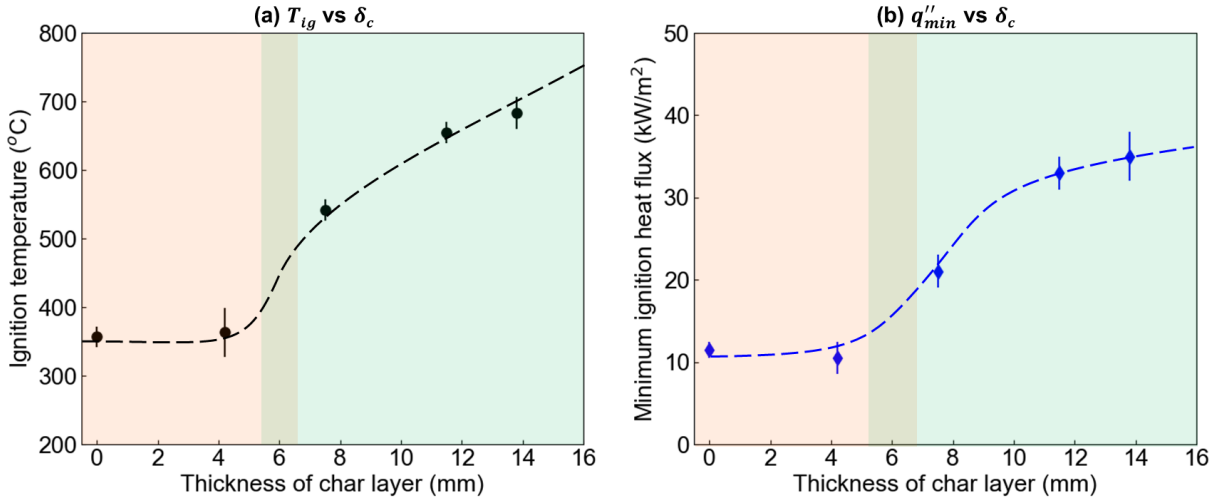

Fig. 7. (a) The measured ignition temperatures and (b) the calculated minimum ignition irradiation based on Eq. 3 for engineered wood with different char-layer thicknesses.

There is also expected to be a different makeup of the charred layer depending on heating duration. When the pre-heating/charring duration is short, there are still virgin wood components remaining in the black pre-charred layer. Therefore, both the ignition time and minimum irradiation remain the same as the virgin wood. By increasing the pre-charring duration and thickness (above 6 mm), eventually, rare virgin wood components remain in the top surface char layer, as illustrated in Fig. 8. Then, the surface char layer acts as an effective thermal insulator to delay the temperature increase and pyrolysis of the underlying virgin wood. Therefore, increased thermal irradiation for a longer duration is required, raising the internal temperature via heat conduction through the surface layer to form a robust internal pyrolysis front, but ultimately resulting in a higher surface temperature along the pre-charred layer at the time of ignition.

Assuming that there is no virgin wood component remaining in the charred layer, the required in-depth heat conduction can be estimated under thermal equilibrium as

$$\dot{q}''_{cond} \approx k_C \frac{T_{ig} - T_{py}}{\delta_C} = \dot{q}''_{ir} - \dot{q}''_{loss} \tag{4}$$

where $T_{py} \approx 300$ °C is the pyrolysis temperature of the virgin wood (see TGA in the Appendix), δ_C and k_C are the thickness and thermal conductivity of the char layer. In short, the (surface) ignition temperature for the pre-charred wood can be estimated as

$$T_{ig} \approx \begin{cases} T_{py} & (\delta_C \leq 6 \text{ mm}) \\ T_{py} + \dfrac{\delta_C}{k_C}(\dot{q}''_{ir} - \dot{q}''_{loss}) & (\delta_C > 6 \text{ mm}) \end{cases} \tag{5}$$

which agrees with the experimental observation in Fig. 7(a). Note that when there is a thick char layer ($\delta_C > 6$ mm), the ignition temperature is not constant but changes with the irradiation level.

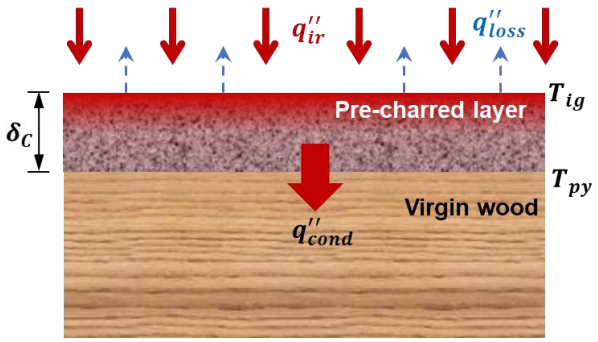

Fig. 8. Heat transfer diagram of the pre-charred wood.

3.4. Fire heat release rate

In terms of the fire hazard, the heat release rate (HRR) or heat release rate per unit area (HRRPUA) is an important parameter, alongside the fire spread rate and structural fire resilience. Based on the principle of oxygen calorimetry, the HRRPUA ($\dot{Q}''$) can be calculated to quantify the intensity of a flame as

$$\dot{Q}'' = (0.21 - X_{O_2}) V_a \rho_{O_2} \Delta H_{ox} / A \tag{6}$$

where V_a is the volumetric flow rate of air, ρ_{O_2} is the density of oxygen at standard temperature and pressure, X_{O_2} is the mole fraction of oxygen in the 'scrubbed' gases, $\Delta H_{ox} \approx 13.1$ MJ/kg is the heat of oxidation of hydrocarbon-based fuel, and A is the cross-sectional area of the sample.

Figure 9 compares the evolution of HRRPUA of virgin wood and pre-charred wood with a char layer of 7.5 mm under irradiations of (a) 40 kW/m^2 and (b) 50 kW/m^2. For the virgin wood (blue dashed line), the HRRPUA curve is similar to the typical time evolution shown in [35], where two peaks are observed before the extinction of the flame. Specifically, for the virgin wood, the HRRPUA increases

immediately to a peak value of about 135 kW/m^2 right after the flame appears and then decreases due to the build-up of a self-formed char layer on the top surface. Continuing heating, the pyrolysis front gradually reaches the bottom of the wood sample and approaches the top of the insulation board, so that the in-depth heat conduction inside the wood is reduced. As a result, the temperature inside the wood sample is increased, and the rate of pyrolysis is accelerated, resulting in a larger flame and the second peak HRRPUA of about 100 kW/m^2. Afterwards, the whole sample surface is mostly charred, and the flame is extinguished while the HRRPUA witnesses a sharp decrease.

For the curve of the HRRPUA of the pre-charred wood with a 7.5-mm char layer (orange solid line), compared with that of virgin wood, the first peak HRRPUA decreases by more than half from around 135 kW/m^2 to 50 kW/m^2 under an irradiation of 40 kW/m^2 (Fig. 9a), and from around 175 kW/m^2 to 75 kW/m^2 under an irradiation of 50 kW/m^2 (Fig. 9b), which are consistent with the experimental phenomena where the flame becomes weaker above the pre-charred woods (Fig. 4). As the flame becomes weaker, the reduced flame heat flux contributes to the decrease in the heat release rate and mass loss rate (Fig. 10) [59,70]. However, the second peak HRRPUA is not very sensitive to the existence of the pre-charred layer, because the second peak is a manifestation of thermal penetration on the back of the sample which is not related to the pre-charring process.

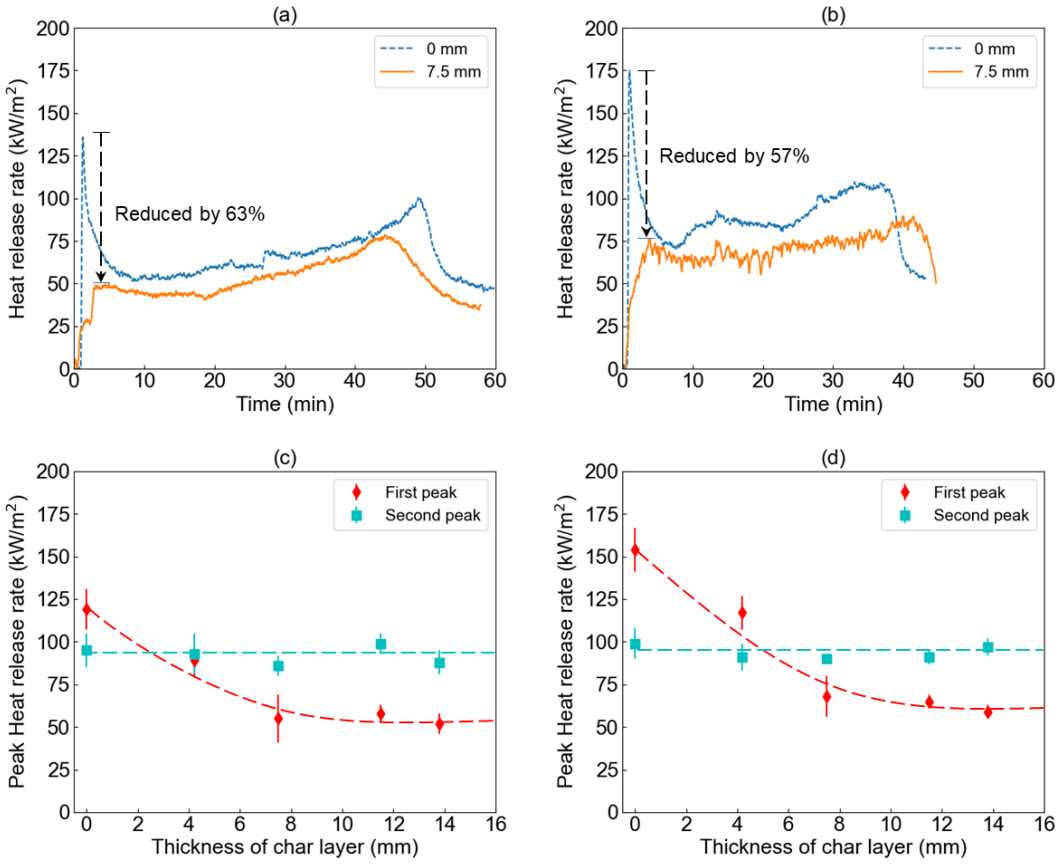

Fig. 9. Comparisons of the evolution of fire HRRPUA of virgin and pre-charred wood with a 7.5-mm char layer under irradiation of (a) 40 kW/m^2 and (b) 50 kW/m^2, and a summary of the two peak HRRPUA found under (c) 40 kW/m^2 and (d) 50 kW/m^2.

Figure 9 (c-d) further summarises the first and second peaks of the HRRPUAs of the virgin and pre-charred woods under irradiations of (c) 40 kW/m^2 and (d) 50 kW/m^2. First, the first peak HRRPUA decreases as the thickness of the char layer increases, showing better fire retardancy and lower flammability of the pre-charred wood. For example, under an irradiation of 50 kW/m^2, as the thickness of the pre-charred layer increases from 0 mm to 13.8 mm, the first peak HRRPUA decreases remarkably by around two-thirds from 155 kW/m^2 to 59 kW/m^2. For the second peak HRRPUA, it remains constant at around 90 kW/m^2 and 100 kW/m^2 under irradiations of 40 kW/m^2 and 50 kW/m^2.

3.5. Burning mass flux

The mass flux or mass loss rate per unit area is another criterion to quantify the burning behaviour of building materials, which is computed as the time derivative of the sample mass measurements. Fig. 10(a-b) illustrates the time evolutions of mass flux under 40 kW/m^2 and 50 kW/m^2 of the same tests in Fig. 9(a-b). As expected, the mass flux generally follows the same trend as the HRR, and the first peak mass flux of wood with a 7.5-mm char layer decreased by over 50% compared to that of the virgin wood.

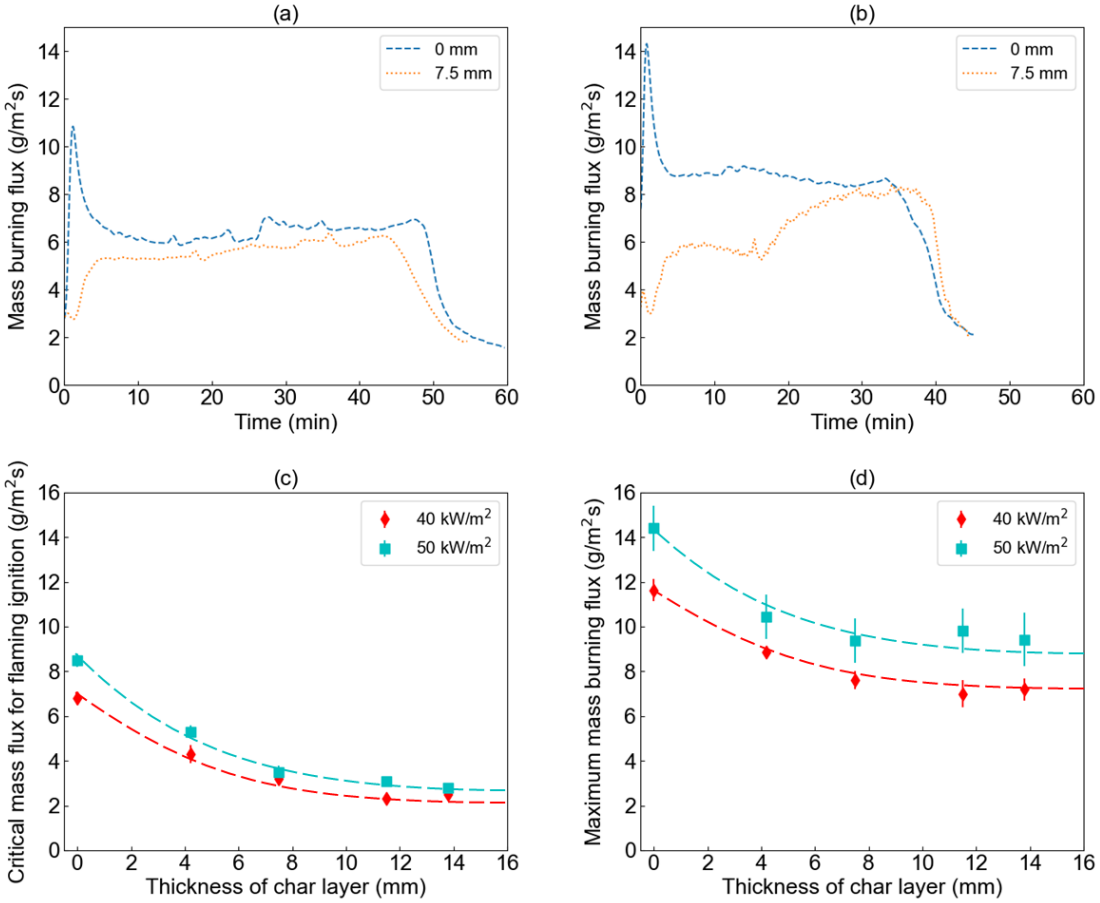

Fig. 10. Mass burning flux of virgin wood and 7.5-mm charred wood under irradiation of (a) 40 kW/m^2 and (b) 50 kW/m^2, (c) critical mass flux for flaming ignition, and (d) maximum mass flux.

Figure 10(c) further summarises the critical mass flux for flaming ignition, a potential criterion for ignition [71] where it increases as the heat flux increases, well agreeing with the trend in the literature [72]. More importantly, the critical mass flux experiences a decrease as the thickness of the char layer increases. For example, given an irradiation of 40 kW/m^2, as the pre-charred layer increases from 0 mm to 13.8 mm, the critical mass flux decreases from 8.1 g/m^2-s to 2.7 g/m^2-s, agreeing with evidence of a weaker flame above the pre-charred wood at the ignition moment (Fig. 4). Furthermore, the maximum burning mass flux also decreases as the thickness of the char layer increases, as shown in Fig. 10(d). Therefore, the burning rate of the inner virgin wood is decelerated which may help maintain its integrity and prevent structural failure during fire accidents.

In summary, we have demonstrated that the pre-charring process could significantly improve the fire performance of the engineered wood materials. For the tested wood species (Merbau wood), the minimum thickness of an effective pre-charred layer is found to be 6 ± 1 mm, which should be larger than the thermal penetration depth of the virgin wood at the ignition moment. An effective char layer could increase the thermal inertia of wooden materials, leading to improved fire performance by increasing required ignition times and ignition temperatures. The observed flame intensity above the pre-charred surface is also weakened, as further demonstrated by the peak HRRPUAs that could be reduced by over 50%. The peak mass flux also decreases as the thickness of the char layer increases, which may help delay structural failure due to the mass loss of structural members during fire accidents. Note that critical values presented here are limited to the specific bench-scale test setup, thus more investigations at different scales are necessary to further understand the flammability, fire performance and resilience of pre-charred woods.

4. Conclusions

This work applies a novel and low-cost method to generate a uniform insulating pre-charred layer over virgin wood using a low irradiation of 20 kW/m^2. The thickness of the char layer is found to increase linearly with a constant charring rate of ~0.7 mm/min. For the studied wood (Merbau), we found the minimum thickness of an effective pre-charred layer to be 6 ± 1 mm, which should be larger than the thermal penetration depth of the virgin wood. Compared with virgin wood, an effective char layer could remarkably increase the thermal inertia of the pre-charred wood. The difficulty in igniting the pre-charred wood significantly increases in terms of the ignition delay time, ignition temperature, and minimum irradiation. For example, with a 13.8-mm char layer, under an irradiation of 40 kW/m^2, the required ignition time increases by seven-fold to 272 s, and the ignition temperature increases above 670 ^{o}C.

After ignition, the fire hazards of the pre-charred woods are also mitigated significantly. As the thickness of the pre-charred layer increases, the flame gradually becomes weak, thin, flat, blue and discrete such that it appears to float above the hot charred surface, different from the typically intense yellow flames found over virgin wood under the same heating conditions. The peak heat release rate of

the pre-charred wood is also reduced by up to 50% compared with that of virgin wood. The peak mass flux of the pre-charred wood is similarly decreased, helping maintain the integrity and prevent structural failure in real fire scenarios. This work provides a promising approach to lowering the flammability and improving the fire performance of wooden materials, which may pave a way for the popularisation of wooden buildings for future carbon-neutral construction. Future work will examine other properties essential for future applications, including durability, surface, structural and mechanical properties.

Declaration of Competing Interest

The authors declare no conflict of interest.

CRediT authorship contribution statement

Shaorun Lin: Investigation, Writing-original draft, Methodology, Formal analysis, Resources. **Yunzhu Qin**: Investigation, Resources. **Xinyan Huang**: Conceptualization, Methodology, Supervision, Formal analysis, Writing-review & editing, Funding acquisition. **Michael Gollner:** Supervision, Resources, Writing-review & editing.

Acknowledgements

This work is funded by the National Natural Science Foundation of China (NSFC) No. 51876183 and the Joint Postdoc Scheme of the Hong Kong Polytechnic University and the University of California at Berkeley (No. P0038960).

References

[1] Karlen C. Multiple Scales Insight into Using Timber for a Sustainable and Future Approach to Buildings. In: Sayigh A, editor. The Importance of Wood and Timber in Sustainable Buildings, Switzerland: Springer Nature; 2021, p. 195–211. https://doi.org/10.1007/978-3-030-71700-1_8.

[2] Kim DH, Na IY, Jang HK, Kim HD, Kim GT. Anisotropic electrical and thermal characteristics of carbon nanotube-embedded wood. Cellulose 2019;26:5719–30. https://doi.org/10.1007/s10570-019-02485-y.

[3] Beasley W. The Japanese Experience: A Short History of Japan. California: University of California Press; 1999.

[4] Wang J, Wang L, Gardner DJ, Shaler SM, Cai Z. Towards a cellulose-based society: opportunities and challenges. vol. 28. Springer Netherlands; 2021. https://doi.org/10.1007/s10570-021-03771-4.

[5] Tollefson J. Wood Grows Up. Nature 2017;545:280–2. https://doi.org/10.1038/545280a.

[6] Barber D. Tall Timber Buildings: What's Next in Fire Safety ? Fire Technology 2015;51:1279–84. https://doi.org/10.1007/s10694-015-0497-7.

[7] Bowyer J, Bratkovich S, Howe J, Fernholz K, Frank M, Hanessian S, et al. Modern Tall Wood Buildings: Opportunities for Innovation. Dovetail Partners Inc 2015:16.

[8] Chen C, Kuang Y, Zhu S, Burgert I, Keplinger T, Gong A, et al. Structure–property–function relationships of natural and engineered wood. Nature Reviews Materials 2020:19–21. https://doi.org/10.1038/s41578-020-0195-z.

[9] Mitchell H, Thomson D, Richter F, Barber D, Rein G. Review of fire experiments in mass timber compartments : Current understanding , limitations , and research gaps 2022:1–18. https://doi.org/10.1002/fam.3121.

[10] Ahn N, Dodoo A, Riggio M, Muszynski L, Schimleck L, Puettmann M. Circular economy in mass

timber construction: State-of-the-art, gaps and pressing research needs. Journal of Building Engineering 2022;53:104562. https://doi.org/10.1016/j.jobe.2022.104562.

[11] Wimmers G. Wood: A construction material for tall buildings. Nature Reviews Materials 2017;2:1–3. https://doi.org/10.1038/natrevmats.2017.51.

[12] Stoeckel F, Konnerth J, Gindl-Altmutter W. Mechanical properties of adhesives for bonding wood-A review. International Journal of Adhesion and Adhesives 2013;45:32–41. https://doi.org/10.1016/j.ijadhadh.2013.03.013.

[13] Ayanleye S, Udele K, Nasir V, Zhang X, Militz H. Durability and protection of mass timber structures: A review. Journal of Building Engineering 2022;46:103731. https://doi.org/10.1016/j.jobe.2021.103731.

[14] Wang D, Lin L, Fu F. Deformation mechanisms of wood cell walls under tensile loading: a comparative study of compression wood (CW) and normal wood (NW). Cellulose 2020;27:4161–72. https://doi.org/10.1007/s10570-020-03095-9.

[15] Lu Y, Feng M, Zhan H. Preparation of SiO2–wood composites by an ultrasonic-assisted sol–gel technique. Cellulose 2014;21:4393–403. https://doi.org/10.1007/s10570-014-0437-6.

[16] Vaks A, Mason AJ, Breitenbach SFM, Kononov AM, Osinzev A V., Rosensaft M, et al. Palaeoclimate evidence of vulnerable permafrost during times of low sea ice. Nature 2020;577:221–5. https://doi.org/10.1038/s41586-019-1880-1.

[17] Wang K, Wang S, Meng D, Chen D, Mu C, Li H, et al. A facile preparation of environmentally-benign and flame-retardant coating on wood by comprising polysilicate and boric acid. Cellulose 2021;28:11551–66. https://doi.org/10.1007/s10570-021-04238-2.

[18] Yang WJ, Wei CX, Yuen ACY, Lin B, Yeoh GH, Lu HD, et al. Fire-retarded nanocomposite aerogels for multifunctional applications: A review. Composites Part B: Engineering 2022;237:109866. https://doi.org/10.1016/j.compositesb.2022.109866.

[19] Richter F, Jervis FX, Huang X, Rein G. Effect of oxygen on the burning rate of wood. Combustion and Flame 2021;234:111591. https://doi.org/10.1016/j.combustflame.2021.111591.

[20] Xing Z, Wang Y, Zhang J, Ma H. Comparative study on fire resistance and zero strength layer thickness of CLT floor under natural fire and standard fire. Construction and Building Materials 2021;302:124368. https://doi.org/10.1016/j.conbuildmat.2021.124368.

[21] Jiang L, Zhao Z, Tang W, Miller C, Sun JH, Gollner MJ. Flame spread and burning rates through vertical arrays of wooden dowels. Proceedings of the Combustion Institute 2019;37:3767–74. https://doi.org/10.1016/j.proci.2018.09.008.

[22] Wang S, Ding P, Lin S, Gong J, Huang X. Smoldering and Flaming of Disc Wood Particles Under External Radiation: Autoignition and Size Effect. Frontiers in Mechanical Engineering 2021;7:1–11. https://doi.org/10.3389/fmech.2021.686638.

[23] Liang Z, Lin S, Huang X. Smoldering ignition and emission dynamics of wood under low irradiation. Fire and Materials 2022:1–11. https://doi.org/10.1002/fam.3107.

[24] Gong J, Yang L. A Review on Flaming Ignition of Solid Combustibles: Pyrolysis Kinetics, Experimental Methods and Modelling. Springer US; 2022. https://doi.org/10.1007/s10694-022-01339-7.

[25] Engel T, Werther N. Structural Means for Fire-Safe Wooden Façade Design. Fire Technology 2021. https://doi.org/10.1007/s10694-021-01174-2.

[26] Kallada Janardhan R, Hostikka S. Predictive Computational Fluid Dynamics Simulation of Fire Spread on Wood Cribs. Fire Technology 2019;55:2245–68. https://doi.org/10.1007/s10694-019-00855-3.

[27] Atreya A. Ignition of fires. Philosophical Transactions of the Royal Society A: Mathematical, Physical and Engineering Sciences 1998;356:2787–813. https://doi.org/10.1098/rsta.1998.0298.

[28] Lineham SA, Thomson D, Bartlett AI, Bisby LA, Hadden RM. Structural response of fire-exposed cross-laminated timber beams under sustained loads. Fire Safety Journal 2016;85:23–34. https://doi.org/10.1016/j.firesaf.2016.08.002.

[29] Wang S, Ding P, Lin S, Huang X, Usmani A. Deformation of wood slice in fire: Interactions between heterogeneous chemistry and thermomechanical stress. Proceedings of the Combustion Institute 2021;38:5081–90. https://doi.org/10.1016/j.proci.2020.08.060.
[30] Cuevas J, Torero JL, Maluk C. Flame extinction and burning behaviour of timber under varied oxygen concentrations. Fire Safety Journal 2020:23. https://doi.org/10.1016/j.firesaf.2020.103087.
[31] Emberley R, Inghelbrecht A, Yu Z, Torero JL. Self-extinction of timber. Proceedings of the Combustion Institute 2017;36:3055–62. https://doi.org/10.1016/j.proci.2016.07.077.
[32] Emberley R, Do T, Yim J, Torero JL. Critical heat flux and mass loss rate for extinction of flaming combustion of timber. Fire Safety Journal 2017;91:252–8. https://doi.org/10.1016/j.firesaf.2017.03.008.
[33] Lin S, Huang X. Extinction of Wood Fire: Modeling Smoldering and Near-Limit Flame Under Irradiation. Fire Technology 2022. https://doi.org/10.1007/s10694-022-01295-2.
[34] Bartlett AI, Hadden RM, Hidalgo JP, Santamaria S, Wiesner F, Bisby LA, et al. Auto-extinction of engineered timber: Application to compartment fires with exposed timber surfaces. Fire Safety Journal 2017;91:407–13. https://doi.org/10.1016/j.firesaf.2017.03.050.
[35] Lin S, Huang X, Gao J, Ji J. Extinction of Wood Fire: A Near-Limit Blue Flame Above Hot Smoldering Surface. Fire Technology 2022;58:415–34. https://doi.org/10.1007/s10694-021-01146-6.
[36] Arnórsson SM, Hadden RM, Law A. The Variability of Critical Mass Loss Rate at Auto-Extinction. Fire Technology 2020. https://doi.org/10.1007/s10694-020-01002-z.
[37] LeVan SL, Jerrold. E. W. Effects of fire-retardant treatments on wood strength: a review. Wood and Fiber Science 2007;22:113–31.
[38] Ilhan F, Kıyan E, Yüzer N. Use of sheep slaughterhouse-derived struvite in the production of environmentally sustainable cement and fire-resistant wooden structures 2022;366. https://doi.org/10.1016/j.jclepro.2022.132948.
[39] Zhou X, Fu Q, Zhang Z, Fang Y, Wang Y, Wang F, et al. Efficient flame-retardant hybrid coatings on wood plastic composites by layer-by-layer assembly. Journal of Cleaner Production 2021;321:128949. https://doi.org/10.1016/j.jclepro.2021.128949.
[40] Jiang T, Feng X, Wang Q, Xiao Z, Wang F, Xie Y. Fire performance of oak wood modified with N-methylol resin and methylolated guanylurea phosphate/boric acid-based fire retardant. Construction and Building Materials 2014;72:1–6. https://doi.org/10.1016/j.conbuildmat.2014.09.004.
[41] Jiang J, Li J, Hu J, Fan D. Effect of nitrogen phosphorus flame retardants on thermal degradation of wood. Construction and Building Materials 2010;24:2633–7. https://doi.org/10.1016/j.conbuildmat.2010.04.064.
[42] Popescu CM, Pfriem A. Treatments and modification to improve the reaction to fire of wood and wood based products—An overview. Fire and Materials 2020;44:100–11. https://doi.org/10.1002/fam.2779.
[43] Uddin M, Kiviranta K, Suvanto S, Alvila L, Leskinen J, Lappalainen R, et al. Casein-magnesium composite as an intumescent fire retardant coating for wood. Fire Safety Journal 2020;112:102943. https://doi.org/10.1016/j.firesaf.2019.102943.
[44] Gaff M, Kačík F, Gašparík M, Todaro L, Jones D, Corleto R, et al. The effect of synthetic and natural fire-retardants on burning and chemical characteristics of thermally modified teak (Tectona grandis L. f.) wood. Construction and Building Materials 2019;200:551–8. https://doi.org/10.1016/j.conbuildmat.2018.12.106.
[45] Sun L, Xie Y, Ou R, Guo C, Hao X, Wu Q, et al. The influence of double-layered distribution of fire retardants on the fire retardancy and mechanical properties of wood fiber polypropylene composites. Construction and Building Materials 2020;242:118047. https://doi.org/10.1016/j.conbuildmat.2020.118047.
[46] Zhang L, Liang S, Chen Z. Influence of particle size and addition of recycling phenolic foam on mechanical and flame retardant properties of wood-phenolic composites. Construction and Building Materials 2018;168:1–10. https://doi.org/10.1016/j.conbuildmat.2018.01.173.

[47] Nasirzadeh M, Yahyaei H, Mohseni M. Effects of inorganic fillers on the performance of the water-based intumescent fire-retardant coating. Fire and Materials 2022:1–11. https://doi.org/10.1002/fam.3067.
[48] Sevda BT, Ayfer DC, Turgay O. The synergistic effect of intumescent coating containing titanium dioxide and antimony trioxide onto spruce and alder wood species. Journal of Building Engineering 2020;31:101407. https://doi.org/10.1016/j.jobe.2020.101407.
[49] Yasemin A, Doğan M, Bayramlı E. The effect of red phosphorus on the fire properties of intumescent pine wood flour – LDPE composites Yasemin. Finnish-Swedish Flame Days 2009 2009;40:4B. https://doi.org/10.1002/fam.
[50] Rowell RM. Chemical modification of wood: A short review. Wood Material Science and Engineering 2006;1:29–33. https://doi.org/10.1080/17480270600670923.
[51] Hasburgh LE, Zelinka SL, Bishell AB, Kirker GT. Durability and fire performance of charred wood siding (Shou sugi ban). Forests 2021;12. https://doi.org/10.3390/f12091262.
[52] Machová D, Oberle A, Zárybnická L, Dohnal J, Šeda V, Dömény J, et al. Surface characteristics of one-sided charred beech wood. Polymers 2021;13:1–15. https://doi.org/10.3390/polym13101551.
[53] Gaff M, Babiak M, Kačík F, Sandberg D, Turčani M, Hanzlík P, et al. Plasticity properties of thermally modified timber in bending – The effect of chemical changes during modification of European oak and Norway spruce. Composites Part B: Engineering 2019;165:613–25. https://doi.org/10.1016/j.compositesb.2019.02.019.
[54] Hein C. Shaping Tokyo: Land development and planning practice in the early modern Japanese metropolis. Journal of Urban History 2010;36:447–84. https://doi.org/10.1177/0096144209347737.
[55] Kymäläinen M, Hautamäki S, Lillqvist K, Segerholm K, Rautkari L. Surface modification of solid wood by charring. Journal of Materials Science 2017;52:6111–9. https://doi.org/10.1007/s10853-017-0850-y.
[56] Kymäläinen M, Turunen H, Čermák P, Hautamäki S, Rautkari L. Sorption-related characteristics of surface charred spruce wood. Materials 2018;11. https://doi.org/10.3390/ma11112083.
[57] Gupta M, Yang J, Roy C. Specific heat and thermal conductivity of softwood bark and softwood char particles.Fuel 2003;82:919–27.
[58] Klippel M, Schmid J. Design of cross-laminated timber in fire. Structural Engineering International 2017;27:224–30. https://doi.org/10.2749/101686617X14881932436096.
[59] Morrisset D, Hadden RM, Bartlett AI, Law A, Emberley R. Time dependent contribution of char oxidation and flame heat feedback on the mass loss rate of timber. Fire Safety Journal 2021;120:103058. https://doi.org/10.1016/j.firesaf.2020.103058.
[60] Gan W, Chen C, Wang Z, Song J, Kuang Y, He S, et al. Dense, Self-Formed Char Layer Enables a Fire-Retardant Wood Structural Material. Advanced Functional Materials 2019;29:1–9. https://doi.org/10.1002/adfm.201807444.
[61] Babrauskas V. The Cone Calorimeter. In: Hurley M, editor. SFPE Handbook of Fire Protection Engineering. 5th Editio, London: Springer; 2016, p. 952–80. https://doi.org/10.1007/978-1-4939-2565-0.
[62] Dutta S, Kim NK, Das R, Bhattacharyya D. Effects of sample orientation on the fire reaction properties of natural fibre composites. Composites Part B: Engineering 2019;157:195–206. https://doi.org/10.1016/j.compositesb.2018.08.118.
[63] Li K, Hostikka S, Dai P, Li Y, Zhang H, Ji J. Charring shrinkage and cracking of fir during pyrolysis in an inert atmosphere and at different ambient pressures. Proceedings of the Combustion Institute 2017;36:3185–94. https://doi.org/10.1016/j.proci.2016.07.001.
[64] Li K, Mousavi M, Hostikka S. Char cracking of medium density fibreboard due to thermal shock effect induced pyrolysis shrinkage. Fire Safety Journal 2017;91:165–73. https://doi.org/10.1016/j.firesaf.2017.04.027.
[65] Qin R, Zhou A, Chow CL, Lau D. Structural performance and charring of loaded wood under fire. Engineering Structures 2021;228:111491. https://doi.org/10.1016/j.engstruct.2020.111491.

[66] Quintiere JG. Fundamentals of fire phenomena. John Wiley; 2006. https://doi.org/10.1002/0470091150.
[67] Lin S, Huang X, Urban J, McAllister S, Fernandez-Pello C. Piloted Ignition of Cylindrical Wildland Fuels Under Irradiation. Frontiers in Mechanical Engineering 2019;5. https://doi.org/10.3389/fmech.2019.00054.
[68] Incropera FP. Principles of heat and mass transfer. John Wiley; 2007.
[69] Huang X, Gao J. A review of near-limit opposed fire spread. Fire Safety Journal 2021;120:103141. https://doi.org/10.1016/j.firesaf.2020.103141.
[70] Spearpoint M., Quintiere J. Predicting the burning of wood using an integral model. Combustion and Flame 2000;123:308–25. https://doi.org/10.1016/S0010-2180(00)00162-0.
[71] McAllister S. Critical mass flux for flaming ignition of wet wood. Fire Safety Journal 2013;61:200–6. https://doi.org/10.1016/j.firesaf.2013.09.002.
[72] Rich D, Lautenberger C, Torero JL, Quintiere JG, Fernandez-Pello C. Mass flux of combustible solids at piloted ignition. Proceedings of the Combustion Institute 2007;31 II:2653–60. https://doi.org/10.1016/j.proci.2006.08.055.

Appendix

The wood and char were first pulverised into powders for thermogravimetric analysis. The initial mass of the test samples was about 2-3 mg, and the samples were heated at a constant rate of 30 K/min. Two oxygen concentrations were selected: 0% (nitrogen) and 21% (air), with a flow rate of 50 mL/min. Fig. A1 shows the mass-loss rate (DTG curve) of the (a) virgin wood and (b) pre-charred layer, where the mass is normalised to the original mass of wood. The first peak below 100 °C indicates the water evaporation. For the virgin wood (Fig. A1a), the mass loss rate rapidly increases at about 270 °C, which can be defined as the pyrolysis temperature. For the char layer (Fig. A1b), it no longer has the pyrolysis stage, so it does not release flammable pyrolysis gases to support the flame. The mass loss starts to increase at about 350 °C, which is the minimum temperature for char oxidation. The gas emissions of char oxidation are much less flammable and cannot support a flame.

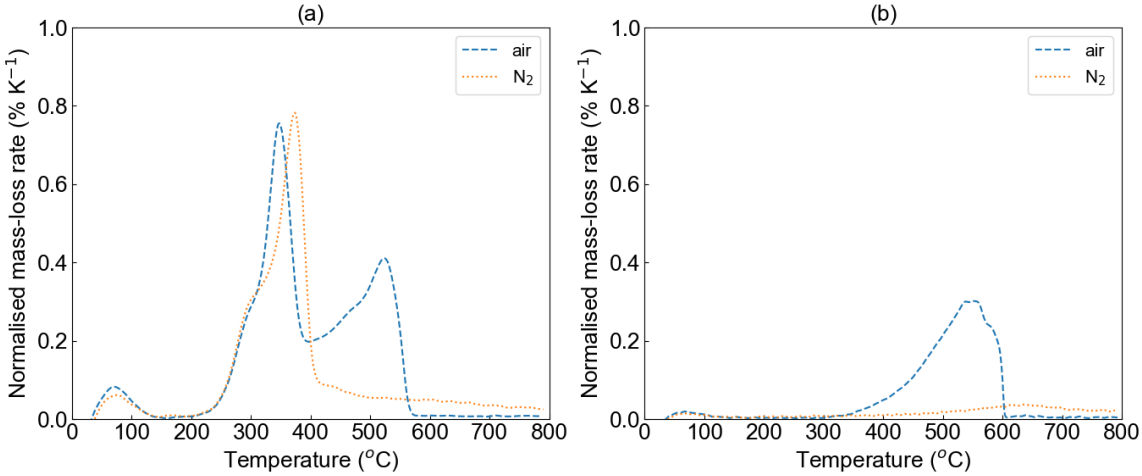

Fig. A1. DTG results of the (a) virgin wood and (b) engineered surface char layer at a heating rate of 30 K/min, where the mass is normalised to the original mass of wood.